Structure and semiconductor properties of titanium suboxide-based composite electrocatalysts

Alexander VELICHENKO[1]*, Vasyl KORDAN[2], Olesia SHMYCHKOVA[1], Valentina KNYSH[1], Pavlo DEMCHENKO[2]

[1] *Ukrainian State University of Chemical Technology, Gagarina Ave. 8, 49005 Dnipro, Ukraine*
[2] *Department of Inorganic Chemistry, Ivan Franko National University of Lviv, Kyryla i Mefodiya St. 6, 79005 Lviv, Ukraine*
* *Corresponding author. Tel.:* +380567462825; *e-mail: velichenko@ukr.net*

Naked Ti/TiO$_2$ nanotubes contain a significant amount of X-ray amorphous compounds on the surface, which are most likely hydrated titanium oxides. The main crystalline phase is titanium dioxide in the allotropic form anatase. Metallic titanium is present on the surface in trace amounts. Thermal treatment of this material at a temperature of 500°C for 3 hours in an air atmosphere led to an increase in the proportion of the crystalline phase. The content of metallic titanium increased significantly, reaching about a third. A partial electrochemical reduction of the nanotubes allowed obtaining more electrically conductive titanium suboxides. After a cathodic reduction of the nanotubes for one hour, a galvanic coating with metallic platinum was uniformly deposited on the surface of the material. Thermally treated Ti/TiO$_2$ nanotubes are an n-type semiconductor with a flat-band potential equal to –0.589 V and a carrier concentration of 6×10^{20} cm^{-3}. Such a high concentration of carriers is obviously due to the small thickness of the oxide film and its non-stoichiometry, as a result of which the surface is not very depleted in electrons, since titanium metal acts as a donor.

Platinized Ti/TiO$_2$ / Nanotubes / Thermal treatment / Charge carriers / Phase composition

1. Introduction

Titanium dioxide is one of the main products of chemical industry. Due to its optical properties, it is widely used in the paint and varnish industry and the production of pigments. Its sensory, adsorption, optical, electrical, and catalytic properties are widely recognized as the objects of close attention of researchers [1].

Due to its high chemical inertness, lack of toxicity, and low cost, titanium dioxide is increasingly used as a photocatalyst, but it has some significant disadvantages: low quantum efficiency of the process due to weak separation of the electron-hole pair, and limited absorption spectrum in the ultraviolet region, which makes it impossible to use the energy of sunlight [2,3]. Scientists in all leading countries of the world are engaged in solving these problems.

It is known that nanosized TiO$_2$ particles (< 50 nm) have the highest photocatalytic activity; therefore, the preparation of TiO$_2$ nanoparticles is one of the ways to reduce the degree of charge recombination and increase the active surface area of the oxide [4].

It is important to note that the addition of dopants into the TiO$_2$ structure can both positively and negatively affect the catalytic activity, so the study of the effect of various additives on the optical and photocatalytic properties of TiO$_2$ is one of the priorities in modern photochemistry. Modern titanium dioxide catalysts obtained in the form of powders have limited application in chemical technology. Therefore, the creation of photocatalytically active coatings with a highly developed surface based on TiO$_2$ is an urgent task, and the development of new methods for their production using nanosized TiO$_2$ particles, as well as ways to modify the resulting material to spatially separate charges in particles and shift the absorption spectrum to lower energies, are promising directions of creating a highly active photocatalyst.

TiO$_2$ nanoparticles are produced with different morphologies, mainly nanotubes, nanowires, nanorods, and mesoporous structures [5]. In recent years, methods such as hydrothermal, solvothermal, sol-gel, direct oxidation methods, chemical vapor deposition, electrodeposition, sonochemical, and microwave methods have been used to produce TiO$_2$ nanoparticles.

For the most part, the catalysts involved are used for cathodic processes. They are relatively stable during operation, but are rapidly destroyed and lose catalytic activity in reverse current or at high anodic polarization, especially in the presence of even small amounts of chloride ions. Under these conditions, there are also problems with current collectors. Carbon materials are rapidly destroyed, and metal and TiO_2 are passivated.

In this paper, we propose to use a combined electrochemical-pyrolytic method of nanotube synthesis. This method will allow one to create a porous developed surface of the matrix for electrodeposition of catalytic layers of platinum and palladium; their subsequent heat treatment at different partial pressures of oxygen will allow one to design composites with different compositions. The high number of cationic vacancies in the matrix and the deficiency of oxygen ions will significantly increase the mobility of platinum and palladium atoms during the heat treatment, and the resulting composite will have practically metal conductivity, high catalytic activity, selectivity, and extended service life.

2. Experimental

All chemicals were analytical reagent grade. Composites were obtained by the original method, which includes stages of preliminary preparation of the titanium substrate [6]. Next, the Ti substance grew enhanced TiO_2 nanotubes following the two-fold anodization and cathodization process [7-9] and galvanic platinization. Platinum was electrodeposited at 80°C at a cathodic current density of 10 mA cm^{-2} from 0.05 M K_2PtCl_6 + 1.5 M $NaNO_2$ + 100 g/L NH_3 [10]. The coating thickness was about 1 μm (∼2 mg Pt per cm^2). Some samples were thermally treated in air, using a tube furnace at 500°C for 1-3 h.

The surface morphology was studied by scanning electron microscopy (SEM) with a Tescan Vega 3 LMU microscope with an energy-dispersive X-ray microanalyzer Oxford Instruments Aztec ONE with X-Max^{N}20 detector. X-ray powder diffraction (XRPD) data were collected in the transmission mode on a STOE Stadi P diffractometer with Cu $K\alpha_1$-radiation (curved Ge (1 1 1) monochromator on the primary beam, $2\theta/\omega$-scan, angular range for data collection 20.000-110.225°2θ with increment 0.015, linear position-sensitive detector with step of recording 0.480°2θ and time per step 75-300 s, $U = 40$ kV, $I = 35$ mA, room temperature. A calibration procedure was performed utilizing SRM 640b (Si) and SRM 676 (Al_2O_3) NIST standards. Preliminary data processing and qualitative phase analysis were performed using STOE WinXPOW and PowderCell program packages. The crystal structures of the phases were refined by the Rietveld method with the program FullProf.2k, applying a pseudo-Voigt profile function and isotropic approximation for the atomic displacement parameters, together with quantitative phase analysis.

The electrochemical measurements were performed in a 1 M solution of $HClO_4$ using a GAMRY Potentiostat / Galvanostat / ZRA Reference 3000 potentiostat in a three-electrode cell with a Pt auxiliary electrode. All potentials were recorded and reported *vs* Ag / AgCl / KCl $_{(sat.)}$. The semiconductor properties of the electrodes were studied by the electrochemical impedance method by measuring the electrode capacity in a 1 M solution of $HClO_4$ at an AC frequency of 5 Hz.

The oxygen evolution reaction was investigated by steady-state polarization on a computer-controlled MTech PGP-550M potentiostat-galvanostat in different electrolytes depending on the purposes of the experiment.

3. Results and discussion

TiO_2 belongs to the class of transition metal oxides and has several modifications: anatase, rutile, brookite, TiO_2(B), TiO_2(II), TiO_2(H) [11,12]. The first three are widespread in Nature. TiO_2(B), with a monoclinic structure, is also found in Nature, but is rare. TiO_2(II) with a PbO_2 structure and TiO_2(H) with a hollandite structure were obtained artificially from rutile under high-pressure conditions. The crystal structures of these polymorphic modifications are based on TiO_6 octahedra. The octahedra are arranged in such a way that they can have common vertices or edges. In anatase, there are four common edges per octahedron; in rutile, there are two. This is the reason for the difference in their characteristics. Titanium dioxide with a brookite structure belongs to the orthorhombic crystal system. In brookite, each octahedron shares edges with two adjacent ones, and these edges are shorter than the others. The unit cell consists of 8 TiO_2 units and is formed from TiO_6 octahedra. Brookite has a more complex crystal structure than anatase or rutile, a larger cell volume, and is also the least dense modification. Anatase and brookite transform into rutile at temperatures of 400-1000°C and ~750°C, respectively [13].

As one can see from Fig. 1, the nanotubes obtained by the method involved here, contain a significant amount of X-ray amorphous material on the surface, which is most likely hydrated titanium oxides. The main crystalline phase is titanium dioxide in the allotropic anatase form. Metallic titanium is present on the surface in trace amounts. Thermal treatment of this material at a temperature of 500°C for 3 h in an air atmosphere led to an increase in the proportion of the crystalline phase (see Fig. 1, Table 1). In this case, the content of metallic titanium increased significantly, reaching about a third. It should be noted that we failed to deposit metallic platinum on the surface of TiO_2 nanotubes obtained by electrolysis. Their heat treatment did also not allow significant progress.

In the best case, local deposition of the coating was observed in certain areas. In this regard, we carried out a partial electrochemical reduction of the nanotubes to obtain more electrically conductive titanium suboxides. A significant amorphization of the surface occurred. Thermal treatment of this sample led to an increase in its crystallinity and an increase in the proportion of metallic titanium in the coating. Thus, as expected, there was a decrease in the proportion of oxygen in the composite material, which should contribute to an increase in the electrical conductivity and an increase in the possibility of applying a metal coating to the surface.

Indeed, after cathodic reduction of the nanotubes for one hour, a galvanic coating with metallic platinum was uniformly deposited on the surface of the material (Fig. 2). Thermal treatment led to an increase in the grain size of the phases and a decrease in microstresses, as well as in the case of nanotubes or reduced nanotubes, to the formation of anatase and an increase in the proportion of metallic titanium in the composite (Table 2).

The semiconducting properties of the obtained materials are of great importance, since they affect the value of the electrode potential under galvanostatic conditions. TiO_2 belongs to semiconductors with a wide band gap. According to literature data, the band gap for the anatase structure is 3.2 eV, brookite 3.3 eV, rutile 3.0 eV [14].
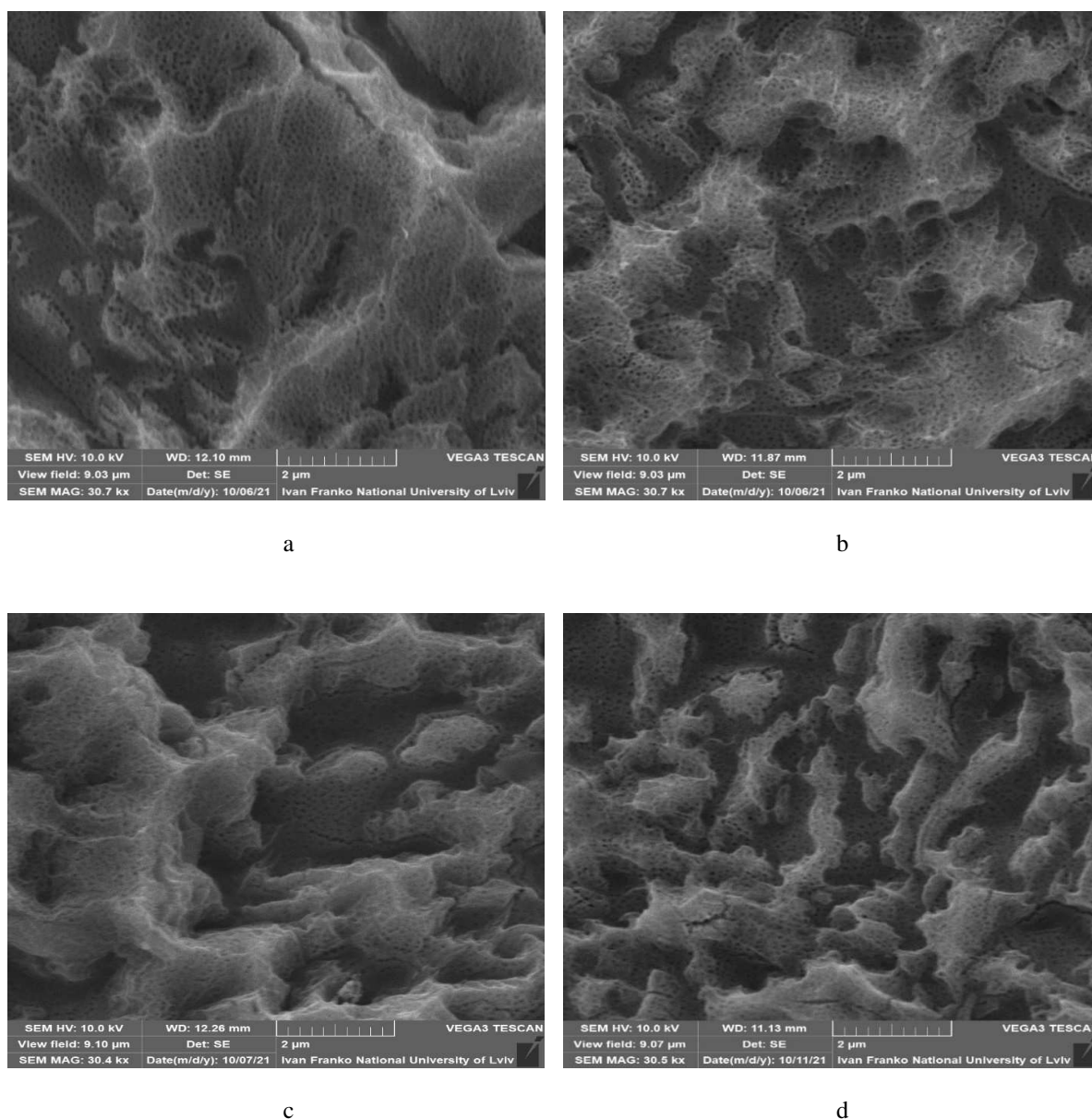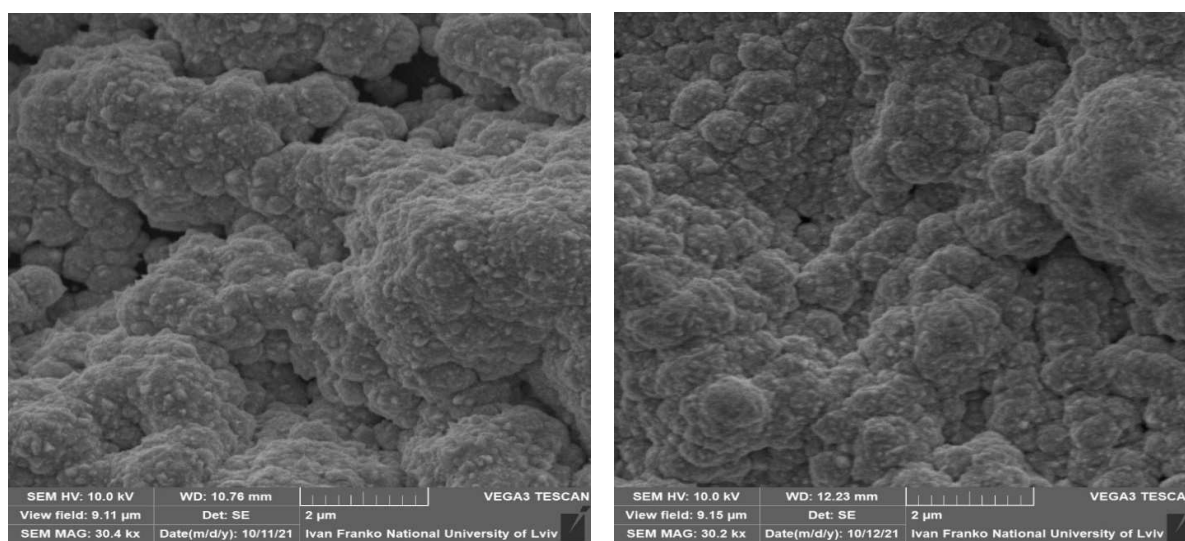

a   b

c   d

Fig. 1 SEM-images of the following surfaces: Ti/TiO$_2$ nanotubes (a); thermally treated Ti/TiO$_2$ nanotubes (b), reduced Ti/TiO$_2$ nanotubes (c), thermally treated reduced Ti/TiO$_2$ nanotubes (d).

Table 1 Phase composition of TiO$_2$ nanotubes treated in various ways.

Material	Phase composition
Ti/TiO$_2$ nanotubes	TiO$_2$ anatase (space group $I4_1/amd$); traces of Ti (structure type Mg, space group $P6_3/mmc$)
Ti/TiO$_2$ nanotubes after thermal treatment	TiO$_2$ anatase 62.7(9) wt.%; Ti 37.3(4) wt.%
Reduced Ti/TiO$_2$ nanotubes	Ti; traces of a phase with a structure of the NaCl type (having in mind SEM/EDAX results it can be TiC$_{1-x}$(O,F)$_x$)
Thermally treated reduced Ti/TiO$_2$ nanotubes	TiO$_2$ anatase 57.6(9) wt.%; Ti 42.4(5) wt.%

Table 2 Phase composition of platinized TiO$_2$ nanotubes treated in various ways.

Material	Phase composition
Reduced Ti/TiO$_2$-Pt nanotubes	Pt 76.9(5) wt.%; Ti 23.1(5) wt.%
Thermally treated reduced Ti/TiO$_2$-Pt nanotubes	Pt 50.6(3) wt.%; Ti 24.4(4) wt.%; TiO$_2$ anatase 25.0(4) wt.%

a

b

Fig. 2 SEM-images of the following surfaces: reduced Ti/TiO$_2$-Pt nanotubes (a); thermally treated reduced Ti/TiO$_2$-Pt nanotubes (b).

The electronic structure of titanium dioxide has been well studied using various approaches [15-17]. The valence band of TiO$_2$ is formed by the outer *p*-electrons of oxygen, and the bottom of the conduction band is predominantly formed by excited titanium ions [14]. The presence of partially reduced titanium (Ti^{3+}) is of particular importance for the electronic properties of titanium dioxide; the level is located ~0.2-0.8 eV below the conduction band [18] and acts as a donor. The presence of Ti^{3+} determines in many cases the conductivity of TiO$_2$.

If in the investigated potential range, the near-surface region of the semiconductor electrode is depleted in basic carriers, then the experimental data obtained by measuring the electrode capacitance should be linear in the coordinates C^{-2}–E and obey the Mott-Schottky equation:

$$C^{-2} = \frac{2}{e\varepsilon\varepsilon_0 N}\left(E - E_{\text{fb}} - \frac{kT}{e}\right) \qquad (1)$$

where C is the electrode capacitance; e is the electron charge, N is the concentration of carriers, E_{fb} is the flat-band potential, k is the Boltzmann constant; T is the absolute temperature, ε and ε_0 are the dielectric constants of the semiconductor and vacuum, respectively.

As preliminary studies have shown, the materials involved are highly doped semiconductors ($N > 10^{18}$ cm^{-3}), and therefore, in the Mott-Schottky equation, it is necessary to take into account the capacity of the Helmholtz layer C_{H}:

$$C^{-2} = C_{\text{H}}^{-2} + \frac{2}{e\varepsilon\varepsilon_0 \text{N}}\left(E - E_{\text{fb}} - \frac{kT}{e}\right) \qquad (2)$$

The slopes of the straight lines in equations (1) and (2) are the same, but in contrast to the value of E_{fb} obtained from (1):

$$E_{\text{fb}} = E_{C^{-2}=0} - \frac{kT}{e} \qquad (3)$$

in the second case we have

$$E_{\text{fb}} = E_{C^{-2}=0} + \frac{e\varepsilon\varepsilon_0 N}{2C_{\text{H}}^{2}} - \frac{kT}{e} \qquad (4)$$

At an alternating current frequency of 5 Hz, the C^{-2}–E dependencies for the materials involved are linear in a wide potential range (R = 0.99). The carrier concentrations were found from the slopes of the straight lines, and the flat-band potentials were found from the intercepts using Eq. (4). The results are presented in Table 3. In all cases, the straight lines are characterized by positive slopes, therefore, the materials involved are n-type semiconductors. With the anodic polarization of such electrodes above the potential of the flat bands, depletion of the number of carriers in the semiconductor will occur. This, in turn, will lead to a decrease in the capacitance of the semiconductor component and, as a result, an increase in the slope of the polarization curve plotted in semilogarithmic coordinates. Thus, an increase in the potential of the flat bands leads to a decrease in the total potential, and an increase in the number of carriers leads to a decrease in the slope of the polarization curve.

For comparison with materials obtained on titanium dioxide nanotubes, we investigated the semiconducting properties of an oxide film obtained on titanium during thermal treatment in a tubular furnace in air at 500°C for three hours. This material is an n-type semiconductor with a flat-band potential equal to –0.589 V and a carrier concentration of 6×10^{20} cm^{-3}. Such a high concentration of

carriers is obviously due to the small thickness of the oxide film and its non-stoichiometry, as a result of which the surface is not very depleted in electrons, since titanium metal acts as an electron donor.

During thermal treatment, the values of the flat-band potential and the concentration of carriers increase, which may be due to the more crystalline structure of the material, which is accompanied by an increase in the proportion of metallic titanium, which acts as an electron donor. A similar phenomenon is observed when a non-continuous platinum coating is applied to the surface of reduced nanotubes. In this case, heat treatment leads to migration of platinum into the bulk of the composite, which, due to its dispersion in the oxide, additionally increases the number of carriers.

The data on the electrocatalytic activity of the obtained materials correlate satisfactorily with the semiconducting properties of the obtained materials (Fig. 3).
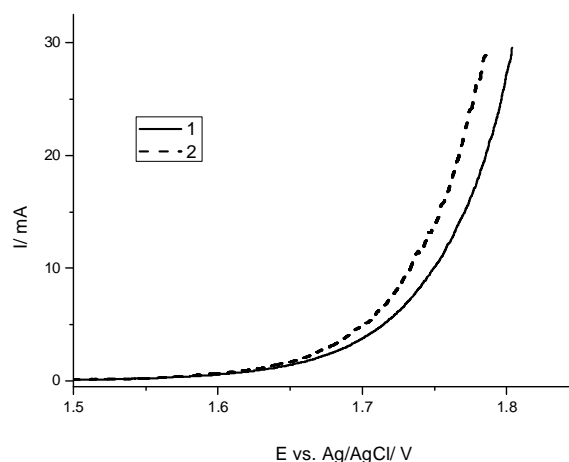

Fig. 3 Quasi steady-state polarization curves for reduced Ti/TiO$_2$-Pt nanotubes (1); thermally treated reduced Ti/TiO$_2$-Pt nanotubes (2).

Conclusions

An original technique, including a stage of thermal treatment of the coating in an air atmosphere, was developed for the deposition of platinized Ti/TiO$_2$ nanotubes. It has been shown that the deposition of platinum on a previously reduced surface of the nanotubes allows one to obtain composite coatings with higher electrical conductivity, and the heat treatment produces a coating characterized by a larger fraction of TiO$_2$, increased adhesion to the current collector, and increased crystallinity. At the same time, the internal stresses of the coating are considerably reduced.

Table 3 Semiconductor properties of TiO_2 nanotubes treated in various ways.

Material	Flat-band potential E_{fb}/ V	Carrier concentration N/ cm^{-3}
Thermally treated Ti/TiO_2 nanotubes	–0.589	6×10^{20}
Ti/TiO_2 nanotubes	0.122	8×10^{22}
Reduced Ti/TiO_2 nanotubes	0.254	1×10^{23}
Thermally treated reduced Ti/TiO_2 nanotubes	0.351	3×10^{23}
Reduced Ti/TiO_2-Pt nanotubes	0.487	6×10^{23}
Thermally treated reduced Ti/TiO_2-Pt nanotubes	0.788	9×10^{23}

References

[1] V.R.A. Ferreira, P.R.M. Santos, C.I.Q. Silva, M.A. Azenha, *Appl. Catal., A* 623 (2021) 118243.

[2] S. Palmas, L. Mais, M. Mascia, A. Vacca, *Curr. Opin. Electrochem.* 28 (2021) 100699.

[3] E. Brillas, *Chemosphere*, 286 (2022) 131849.

[4] M. Bellardita, A. Di Paola, L. Palmisano, F. Parrini, G. Buscarino, R. Amadelli, *Appl. Catal., B* 104 (2011) 291-299.

[5] X. Chen, S.S. Mao, *Chem. Rev.* 107 (2007) 2891-2959.

[6] O. Shmychkova, T. Luk'yanenko, R. Amadelli, A. Velichenko, *J. Electroanal. Chem.* 774 (2016) 88-94.

[7] M. Chen, Sh. Pan, C. Zhang, C. Wang, W. Zhang, Z. Chen, X. Zhao, Yi. Zhao, *Chem. Eng. J.* 399 (2020) 125756.

[8] Y. Yang, M.R. Hoffmann, *Environ. Sci. Technol.* 50 (2016) 11888-11894.

[9] M. Chen, C. Wang, Y. Wang, X. Meng, Z. Chen, W. Zhang, G. Tan, *Electrochim. Acta* 323 (2019) 134779.

[10] O. Kasian, T. Luk'yanenko, A. Velichenko, R. Amadelli, *Int. J. Electrochem. Sci.* 7 (2012) 7915-7926.

[11] P.Y. Simons, F. Dachille, *Acta Crystallog.* 23 (1967) 334-336.

[12] M. Latroche L. Brohan, R. Marchand, M. Tournoux, *J. Solid State Electrochem.* 81 (1989) 78-82.

[13] T.A. Kandiel, L. Robben, A. Alkaimad, D. Bahnemann, *Photochem. Photobiol. Sci.* 12 (2013) 602-609.

[14] M. Landmann, E. Rauls, W.G. Schmidt, *J. Condens. Matter Phys.* 24 (2012) 1-6.

[15] R. Asahi, Y. Taga, W. Mannstadt, A.J. Freeman, *Phys. Rev. B* 61 (2000) 7459-7465.

[16] V. Luca, S. Djajanti, R.F. Howe, *Phys. Rev.* 102 (1998) 10650-10657.

[17] R. Sanjines, H. Tang, H. Berger, F. Gozzo, G. Margaritondo, F.J. Levy, *J. Appl. Phys.* 75 (1994) 2945-2951.

[18] T.L. Thompson, J.T. Yates, *Chem. Rev.* 10 (106) 4428-4453.